Erythrosin B Phosphorescence Monitors Molecular Mobility and Dynamic Site Heterogeneity in Amorphous Sucrose

Linda C. Pravinata, Yumin You, and Richard D. Ludescher
Department of Food Science, Rutgers, The State University of New Jersey, New Brunswick, New Jersey 08901-8520

ABSTRACT Molecular mobility modulates the chemical and physical stability of amorphous biomaterials. This study used steady-state and time-resolved phosphorescence of erythrosin B to monitor mobility in thin films of amorphous solid sucrose as a function of temperature. The phosphorescence intensity (lifetime), emission energy, and red-edge excitation effect were all sensitive to localized molecular mobility on the microsecond timescale in the glass and to more global modes of mobility activated at the glass transition. Blue shifts in the emission spectrum with time after excitation and systematic variations in the phosphorescence lifetime with wavelength indicated that emission originates from multiple sites ranging from short lifetime species with red-shifted emission spectrum to long lifetime species with blue-shifted emission spectrum; the activation energy for nonradiative decay of the triplet state was considerably larger for the blue-emitting species in both the glass and the melt. This study illustrates that phosphorescence from erythrosin B is sensitive both to local dipolar relaxations in the glass as well as more global relaxations in the sucrose melt and provides evidence of the value of phosphorescence as a probe of dynamic site heterogeneity as well as overall molecular mobility in amorphous biomaterials.

INTRODUCTION

The unusual physical properties of amorphous, noncrystalline solids modulate the functional properties of many biological materials including pharmaceuticals (Skrabanja et al., 1994; Towns, 1995; Craig et al., 1999, Carstensen, 2000) and dried and frozen foods (Karel and Saguy, 1991; Slade and Levine, 1995; Roos, 1995; Fennema, 1996; Peleg, 1996) as well as the biological functions of bacterial spores, plant seeds, and even entire organisms during anhydrobiosis (Crowe et al., 1998; Sun et al., 1998; Leopold, 1999; Buitink et al., 2000; Buitink and Olivier, 2004). The propensity of sugar solutions, for example, to harden into amorphous, glassy solids thus forms the basis for the worldwide sugar confection industry as well as the ability of organisms to endure severe desiccation (Crowe et al., 2002; Tunnacliffe and Lapinski, 2003).

Amorphous solids form during physical processes such as rapid cooling of melts or drying of solutions that frustrate formation of a regular crystalline lattice (Zallen, 1983). The intrinsic steric constraints that modulate crystallization of many biomolecules also facilitate formation of amorphous solids; proteins, for example, readily form amorphous rather than crystalline solids, perhaps partly as a result of evolutionary selection (Doye et al., 2004).

Amorphous solids are thermally plastic, being hard, rigid, and brittle at low temperature, and soft, flexible, and pliable at high temperature. The glass transition controls many of the macroscopic properties and applications of the amorphous material. It is a dynamical rather than an order-disorder transition and reflects the onset of translational motion within the amorphous solid: glassy solids are rigid because the molecules can only undergo vibrational and limited rotational motions whereas rubbery solids or melts exhibit macroscopic flow due to the onset of translational motion above the glass transition temperature (T_g) (Zallen, 1983). Mobility within the amorphous solid is typically discussed in terms of the mechanical or dielectric loss peaks detected as a function of temperature or frequency in amorphous polymers (McCrum et al., 1967). The peak at highest temperature for measurements at constant frequency (or lowest frequency for measurements at constant temperature) is labeled α and reflects activation of those large-scale molecular motions (α-relaxations) that underlie the onset of translational motion seen at the glass transition. Transitions within the glass at lower temperature are labeled β and reflect more localized molecular motions (β-relaxations) within the rigid molecular glass (Johari and Goldstein, 1970, 1971).

A number of techniques are available and widely used to characterize the properties and mobility of amorphous biomaterials including dielectric relaxation spectroscopy, differential scanning calorimetry, NMR spectroscopy, and dynamic mechanical thermal analysis. In an elegant series of studies by Richert and colleagues (reviewed in Richert, 2000), phosphorescence emission spectroscopy has been used to monitor the rate of dielectric relaxation around the excited triplet state of luminescent probes doped within supercooled liquids and amorphous solids. The work described here builds upon research of this type.

Phosphorescence spectroscopy is a sensitive, site-specific method that can be used to detect molecular mobility within the local environment of a triplet probe. Depending upon the specific luminescent molecule, the triplet lifetime ranges from microseconds to seconds, thus providing a sensitive

Submitted October 19, 2004, and accepted for publication January 25, 2005.
Address reprint requests to Richard D. Ludescher, Tel.: 732-932-9611 ext. 231; Fax: 732-932-6776; E-mail: ludescher@aesop.rutgers.edu.
© 2005 by the Biophysical Society
0006-3495/05/05/3551/11 $2.00
doi: 10.1529/biophysj.104.054825

signal on timescales suitable for study of matrices in either the glass or the rubber/melt state. Tryptophan phosphorescence, for example, has been used to study the internal mobility of proteins in solution (Papp and Vanderkooi, 1989; Schauerte et al., 1997) and in the solid state (Shah and Ludescher, 1994) on the milliseconds to seconds timescale; the long triplet lifetimes of this probe provide support for the presence of rigid, glassy regions within even fully hydrated proteins.

Erythrosin B (Ery B) (tetra-iodofluorescein) is perhaps the most widely used phosphorescent probe of the molecular mobility of water-soluble and membrane-bound proteins because of its large extinction coefficient and high phosphorescence quantum yield in aqueous solution. In previous studies (Shah and Ludescher, 1995; Ludescher et al., 2001), we have shown its utility as a probe of the molecular mobility of amorphous sucrose powders. We report here a more detailed investigation of how the delayed emission from erythrosin reports on the molecular mobility and dynamic heterogeneity in optically clear thin films of amorphous sucrose; these data clearly show the utility of this molecule to provide insight into both the overall molecular mobility as well as the variations in molecular mobility (dynamic site heterogeneity) within amorphous solid sucrose and other biomaterials.

MATERIALS AND METHODS

Sample preparation

Approximately 20 g of sucrose (99.5% pure; Sigma Chemical, St. Louis, MO) were dissolved in 100 mL of deionized water containing 0.5 g of activated charcoal to remove luminescent impurities. After stirring overnight, the charcoal was removed by vacuum filtration using ashless filter paper (Whatman No. 40, Whatman International, Maidstone, UK), additional charcoal was added, and the process repeated. The purified solution was freeze-dried and then dried thoroughly over P_2O_5 and DrieRite (Xenia, OH) for over one month. Freeze-dried sucrose was hydrated at a ratio of 2 parts by weight of sucrose to 1 part of deionized water to make a final concentration of 65–67 wt % sucrose; concentration was confirmed using a refractometer (NSG Precision Cells, Farmingdale, NY). This sucrose solution was filtered through a 0.2-μm membrane to remove particulates. Ery B (Sigma Chemical) was dissolved in spectrophotometric grade dimethylformamide (DMF) (Aldrich Chemical, Milwaukee, WI) to make a 10-mM stock solution; aliquots from this solution were added to the concentrated sucrose to make solutions with a molar ratio of dye/sucrose of $1{:}10^4$.

To produce glassy sucrose films containing Ery B, 15 μL of a sucrose solution containing Ery B were spread on a quartz slide ($30 \times 13.5 \times 0.6$ mm; custom made by NSG Precision Cells, Farmingdale, NY). Quartz slides were washed overnight with Alconox soap to improve their surface activity for spreading sucrose solutions, then washed with double distilled water, acid, and finally water again. After addition of the sucrose solution, another slide was placed on top of the solution and the slides were drawn horizontally past one another to form a thin film. The solutions on the slides were then warmed under a heat gun (Vidal Sassoon hairdryer) for 5 min to a maximum temperature of ~88°C (measured using a thermocouple probe). This procedure typically made dried amorphous sucrose films ~40-μm thick. The slides were stored at room temperature against P_2O_5 and DrieRite for at least 3 days before any phosphorescence measurements. Attempts to measure the water content of the films using a gravimetric technique were unsuccessful due to the small amount of sucrose (≤5 mg) on each slide; attempts to determine water content using thermal techniques were also unsuccessful due to the difficulty of removing dried sucrose from the slides. We assume that water content is at most a few percent by weight due to the extensive equilibration time and the thinness of the film.

Luminescence measurements

Most luminescence measurements were made using a Cary eclipse fluorescence spectrophotometer (Varian Instruments, Walnut Creek, CA). This instrument uses a high-intensity pulsed lamp and collects intensity in analog mode; data were not collected within the first 0.1 ms to suppress fluorescence coincident with the lamp pulse. Delayed luminescence spectra as a function of time after excitation were collected using a SPEX F1T11i spectrofluorometer (Jobin Yvon, Edison, NJ) equipped with a model 1934D pulsed lamp phosphorimeter. This instrument uses a low-power pulsed Xenon lamp and a gated-delay amplifier to collect emission in a photon-counting mode at defined time delay after the lamp pulse; the width of the lamp pulse necessitated a 0.1-ms dead time for this instrument.

Before phosphorescence measurements, all samples were flushed for at least 15 min with N_2 gas containing <1 ppm of residual O_2 to eliminate O_2 that effectively quenches the triplet state. All measurements were made in triplicate at least. Sample temperature of the cuvette holder was controlled using either a thermoelectric heater/cooler (Varian Instruments) or a water bath (Fischer Scientific, Pittsburgh, PA); the temperature of the sample was measured directly using a thermocouple in the cuvette.

Delayed luminescence emission spectra were collected from 520 to 750 nm (10 nm bandwidth) using excitation of 500 nm (10 nm bandwidth) over the temperature range from 5 to 100°C using an observation window of 3.0 ms and an initial delay of 0.1 ms. Emission from sucrose film or sucrose solution without probe (although low intensity) was subtracted from each spectrum.

Measurements of the effect of excitation wavelength on the phosphorescence emission spectra (red-edge excitation experiments) used excitation at 530 and 560 nm. Phosphorescence emission was collected from 640 to 740 nm using an observation window of 3.0 ms.

For lifetime measurements as a function of temperature, samples were excited at 530 nm (20 nm bandwidth) and emission transients collected at 680 nm (20 nm bandwidth) at selected temperatures ranging from 5 to 100°C. Samples were equilibrated at each new temperature for 1 min for each 1°C increase or decrease in temperature. Intensity decays were collected from each sample during both heating and cooling cycles. Intensity decays were clearly nonexponential and were analyzed using a stretched exponential function widely used to characterize luminescence in a glass (Richert, 2000):

$$I(t) = I(0)\exp[-(t/\tau)^{\beta}] + \text{constant}, \qquad (1)$$

where $I(0)$ is the initial amplitude, τ is the stretched lifetime, and β is an exponent that varies from 0 to 1 and quantifies the nonexponential nature of the decay; β provides a measure of the distribution of lifetimes required to fit the intensity decay. The smaller the value of β, the wider the dispersion in lifetimes (Lindsey and Patterson, 1980). Intensity decay transients were analyzed using a nonlinear least-squares iterative fitting procedure using the program NFIT (Island Products, Galveston, TX); goodness of fit was evaluated by examining R^2 and plots of the modified residuals (plots of the difference between the calculated and the measured intensity divided by the square root of the measured intensity); R^2 for all stretched exponential fits ranged from 0.99 to 1.000 and, more significantly, the modified residuals plots fluctuated randomly about zero amplitude.

Phosphorescence emission spectra measured as a function of the delay time after excitation used an excitation wavelength of 530 nm and emission spectra were collected from 620 to 750 nm. Each spectrum was collected over a 0.5-ms observation window using time delays of 0.1, 0.6, 1.1, 1.6, 2.1, and 2.6 ms after the lamp flash. The center of gravity of the emission

(ν_{cg}) was calculated from the intensity spectrum ($I(\lambda)$, λ in nanometers) summed over the region from 643 to 750 nm using the following equation (Lakowicz, 1999):

$$\nu_{cg} = 10^4 \Sigma I(\lambda)\lambda^{-1}/\Sigma I(\lambda), \quad (2)$$

where the conversion factor of 10^4 converts inverse nanometers to kKaysers (10^3 cm^{-1}).

Measurements of the lifetime of Ery B as a function of excitation wavelength used emission at 680 nm (20 nm bandwidth); excitation was varied from 490 to 560 nm with 10 nm bandwidth. Measurements of lifetime as a function of emission wavelength used excitation at 530 nm (20 nm bandwidth); emission was varied from 640 to 720 nm with 10 nm bandwidth. Samples were equilibrated for 1 min for each 1°C increase in temperature before collecting phosphorescence decay transients.

The energy of the emission maximum (ν_P) and the full width at half maximum of the emission bands were determined by fitting both delayed fluorescence and phosphorescence emission to a log-normal line-shape function (Maroncelli and Fleming, 1987).

$$I(\nu) = I_0 \exp\{-\ln(2)[\ln(1 + 2b(\nu - \nu_P)/\Delta)/b]^2\}. \quad (3)$$

In this equation I_0 is the maximum emission intensity, ν_P is the frequency (in cm^{-1}) of the emission maximum, Δ is a linewidth parameter, and b is an asymmetry parameter (this equation reduces to a Gaussian linewidth when $b = 0$). The bandwidth (full width at half maximum; Γ) of the emission band is related to b and Δ:

$$\Gamma = \Delta\{sinh(b)/b\}. \quad (4)$$

Delayed luminescence spectra collected from 520 to 750 nm were fit using the program NFIT (Island Products) to a sum of distinct log-normal functions (Eq. 3) for delayed fluorescence ($I_{DF}(\nu)$) and phosphorescence ($I_P(\nu)$) in which all fit parameters were independent for each emission band.

Photophysical scheme

Our analysis of the delayed emission is similar to the photophysical scheme for erythrosin outlined by Duchowicz et al. (1998); a brief outline is provided here. After absorption, the first excited singlet state (S_1) decays by intersystem crossing to the first excited triplet state (T_1). We assume that there is no collisional quenching of the triplet state by oxygen under the anoxic conditions of these measurements and that self-quenching due to collisions between dye molecules (Vanderkooi et al., 1987; Duchowicz et al., 1998) is negligible within the extremely viscous amorphous solid. The triplet state thus decays by intersystem crossing to S_0 (k_{TS0}), by phosphorescence (k_{RP}), and by thermally stimulated reverse intersystem crossing to S_1 (k_{TS1}). The total rate constant (k_P) for deexcitation of the triplet state is then:

$$k_P = k_{RP} + k_{TS0} + k_{TS1}. \quad (5)$$

The phosphorescence emission lifetime is given by the standard expression:

$$\tau = k_P^{-1} = (k_{RP} + k_{TS0} + k_{TS1})^{-1}. \quad (6)$$

Comparison of emission intensities for delayed fluorescence (I_{DF}) and phosphorescence (I_P) provides information about the rate constant for reverse intersystem crossing (among other parameters):

$$I_{DF}/I_P = \phi_F k_{TS1}/k_{RP}, \quad (7)$$

where ϕ_F is the quantum yield for fluorescence. This ratio is highly temperature dependent because the rate constant for reverse intersystem crossing is characterized by an Arrhenius dependence:

$$k_{TS1}(T) = k^o_{TS1} \exp(-\Delta E_{TS}/RT), \quad (8)$$

where R is the gas constant, ΔE_{TS} is the effective T_1 to S_1 energy gap, and k^o_{TS1} is the maximum reverse intersystem crossing rate at high temperature. The temperature dependence of the ratio of delayed fluorescence to phosphorescence is thus:

$$I_{DF}(T)/I_P(T) = (\phi_F/k_{RP})k^o_{TS1} \exp(-\Delta E_{TS}/RT). \quad (9)$$

A plot of $\ln(I_{DF}/I_P)$ versus $1/T$, thus, has slope of $-\Delta E_{TS}/R$.

The temperature dependence of the lifetime is due to the temperature dependence of the nonradiative rate constants. In an amorphous solid in the absence of oxygen, the explicit temperature dependence of k_p can be written as:

$$k_P(T) = k_{RP} + k_{TS0}(T) + k_{TS1}(T), \quad (10)$$

where k_{RP} is 41 s^{-1} and constant with temperature (Duchowicz et al., 1998; Lettinga et al., 2000), $k_{TS1}(T)$ has the form of Eq. 8, and $k_{TS0}(T)$ expresses the nonradiative decay rate due to both internal (intrinsic molecular) and external (matrix mobility) factors (Papp and Vanderkooi, 1989).

RESULTS

Delayed emission spectra

The delayed emission spectra of erythrosin B in optically clear amorphous sucrose films at a 10^{-4} erythrosin/sucrose mol ratio exhibited maxima at ~555 and ~675 nm (Fig. 1). The long wavelength emission band reflects phosphorescence from the triplet state whereas the short wavelength emission band reflects delayed (E-type) fluorescence from the singlet state that has been repopulated by reverse intersystem crossing from the triplet state (Parker, 1968). Delayed emission spectra collected over the temperature range from 5 to 100°C showed the decrease in phosphorescence (I_P) and increase in delayed fluorescence (I_{DF}) intensity at higher temperatures expected from a thermally stimulated process (Parker, 1968). The intensity ratio when plotted as a van't Hoff plot of $\ln(I_{DF}/I_P)$ versus $1/T$ (using the maximum emission intensity determined from fitting spectra to a log-normal function; Eq. 3 in Materials and Methods)

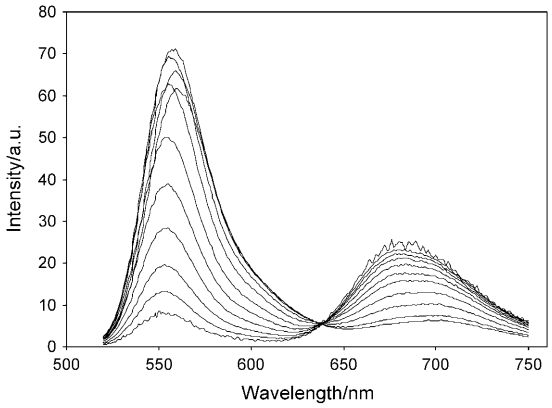

FIGURE 1 Delayed emission spectra of erythrosin B in amorphous sucrose films as a function of temperature (excitation at 500 nm). The spectra were collected at 5, 15, 25, 35, 45, 55, 65, 75, 85, 95, and 100°C (*curves* in order from high to low intensity at 670 nm).

was linear over the entire range of measured temperatures with no systematic deviations ($R^2 \geq 0.998$ for 25 different curves; data not shown); the slope provides an estimate of the energy gap, ΔE_{TS}, between the lowest triplet (T_1) and singlet (S_1) states (Eq. 9 in Materials and Methods). The value of 31.6 ± 0.4 kJ mol^{-1} for ΔE_{TS} in amorphous sucrose was significantly smaller than that measured in water (36.9 ± 0.6 kJ mol^{-1}) or 66 wt % aqueous sucrose (36.9 ± 1.0 kJ mol^{-1}). Further comparison with ΔE_{TS} for erythrosin in ethanol (28.5 ± 2.5 kJ mol^{-1}; Duchowicz et al., 1998) and polyvinyl alcohol (41.2 ± 0.4 kJ mol^{-1}; Lettinga et al., 2000) suggests that solvent (matrix) properties modulate the singlet-triplet energy gap.

The delayed fluorescence exhibited none of the spectral features characteristic of erythrosin aggregates (Pant et al., 1971) and emission spectra collected over a range of erythrosin/sucrose mol ratios from 0.5×10^{-4} to 10×10^{-4} were indistinguishable from those plotted in Fig. 1 and gave indistinguishable values for ΔE_{TS}. Emission lifetimes measured as a function of temperature were also unaffected by varying the probe/sucrose ratios. DMF, the solvent used to prepare erythrosin stock solutions, also did not appear to modulate the spectroscopic properties of erythrosin in amorphous sucrose. Sucrose solutions (66 wt %) with 10^{-4} mol probe ratio were prepared from erythrosin stock solutions at 10 and 100 mM in DMF; despite the resulting 10-fold difference in DMF concentration, the temperature dependence of the emission spectra, red-edge shifts, and lifetimes were identical within error. The spectroscopic properties of erythrosin in amorphous sucrose at a mol ratio of 10^{-4}, thus, reflected the behavior of individual probe molecules dispersed in the sucrose matrix and surrounded by a solvation layer 10–11 sucrose molecules thick.

The delayed fluorescence and phosphorescence bands shifted to longer wavelength (lower energy) at higher temperature. The peak energy (ν_P) and bandwidth (Γ) for both delayed fluorescence and phosphorescence emission were determined by fitting to a log-normal function (Eq. 3). These parameters for phosphorescence are plotted versus temperature in Fig. 2; the peak frequency for delayed fluorescence showed similar behavior whereas the bandwidth was approximately constant over this temperature range. The phosphorescence emission energy decreased linearly in the glass at low temperature and the slope became more negative above the sucrose glass transition temperature ($T_g \approx 65$°C). The decrease in emission energy reflects an increase in the average extent of matrix dipolar relaxation around the excited triplet state before emission (Lakowicz, 1999; Richert, 2000); because the triplet lifetime is also decreasing with temperature (see below), the decrease in average emission energy reflects an increase in the rate of dipolar relaxation in the sucrose melt above T_g.

The phosphorescence bandwidth increased only gradually with temperature in the glass and much more dramatically in the melt above T_g (Fig. 2). This large increase in inhomogeneous broadening indicates that there is a corresponding increase in the width of the distribution of energetically distinct matrix environments in amorphous sucrose above T_g.

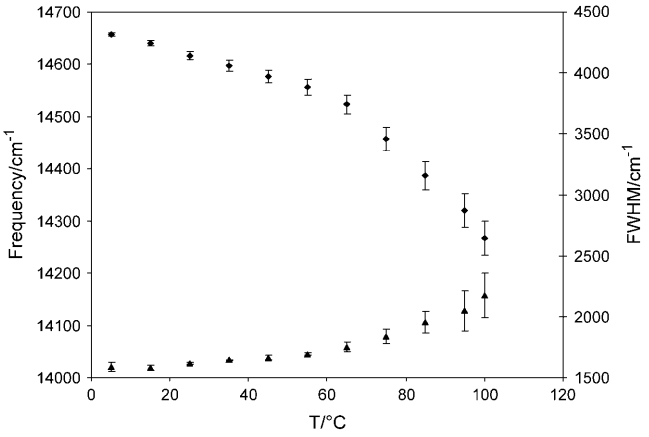

FIGURE 2 Peak energy ν_P (♦, *left* scale) and bandwidth (full-width half maximum) (▲, *right* scale) for phosphorescence emission from erythrosin B in amorphous sucrose film as a function of temperature. Delayed emission spectra collected as a function of temperature were analyzed as described in Materials and Methods using Eq. 3.

Red-edge excitation

The phosphorescence emission energy of erythrosin was sensitive to the excitation wavelength in amorphous solid sucrose. At 5°C the phosphorescence emission maximum was 671 nm with excitation at the absorption maximum of 530 and 689 nm with excitation at the red edge of the absorption band at 560 nm. The ability to photoselect a subpopulation with lower emission energy by using red-edge excitation (Galley and Purkey, 1970; Demchenko, 2002) indicates that some erythrosin probes reside in distinct low-energy environments in the sucrose matrix that persist for periods significantly longer than the triplet state lifetime of ~0.5 ms due to slow matrix relaxation around the excited triplet state.

Measurements of the red-edge effect as a function of temperature in both amorphous sucrose films and in 66 wt% aqueous sucrose are plotted in Fig. 3 as the energy difference with 530 and 560 nm excitation of the center of gravity of the emission band ($\Delta\nu_{cg}$). The magnitude of $\Delta\nu_{cg}$ (which is a direct measure of the magnitude of the red-edge effect) for erythrosin B in amorphous sucrose decreased at higher temperatures. The slope ($d\Delta\nu_{cg}/dT$) was more negative at high than at low temperatures whereas the curve exhibited a break at ~60°C, suggesting that the rate of matrix relaxation increased significantly in the sucrose melt above T_g. The red-edge effect for erythrosin B in 66 wt % aqueous sucrose was essentially zero due to more rapid solvent relaxation within the viscous solution.

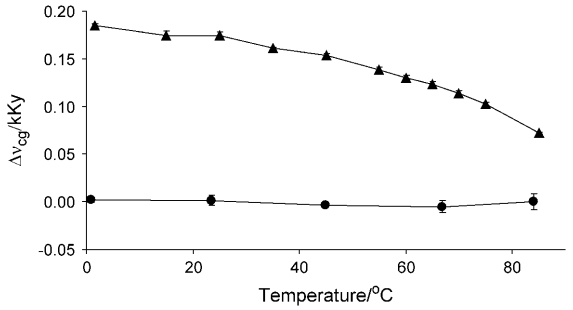

FIGURE 3 The red-edge effect of the phosphorescence emission of erythrosin B plotted as a function of temperature in amorphous sucrose film (▲) and 66 wt % aqueous sucrose (●). The difference in the center of gravity of the emission band (ν_{cg}) of the phosphorescence emission spectra with excitation at 530 and 560 nm is plotted versus temperature.

Phosphorescence decay kinetics

Time-resolved phosphorescence intensity decays of erythrosin B in amorphous sucrose films were measured over the temperature range from 5 to 100°C during both heating and cooling cycles. The phosphorescence intensity decays in sucrose glass at 5 and 85°C, that is, below and above the sucrose T_g, are plotted in Fig. 4 along with fits using a stretched exponential function (Eq. 1 in Materials and Methods). The modified residuals for these fits, included in Fig. 4, varied randomly about zero indicating that the stretched exponential model provided a satisfactory description of the intensity transient over more than two decades of decay in both the sugar glass and the melt (R^2 values for these curves were 0.9998 for the 5°C data and 0.9989 for the 85°C data). All intensity decays at all temperatures were satisfactorily fit using a stretched exponential decay model in which the lifetime (τ) and the stretching exponent (β) were the physically meaningful parameters. Although we reported previously that erythrosin phosphorescence exhibits two lifetimes in a fractured sucrose powder (Shah and Ludescher, 1995), we used a stretched exponential decay model here for several reasons: 1), the stretched exponential model provides a statistically reasonable fit to all measured decays; 2), it provides a simple and tractable way of describing potentially complex decay transients using only two adjustable parameters, τ and β; 3), there are sound theoretical reasons for supposing that rate constants for kinetic processes within an amorphous solid are distributed in a manner appropriate for description by a stretched exponential (Richert, 1997, 1998, 2000); and 4), a number of empirical studies have demonstrated the applicability of the stretched exponential model for describing luminescence decays within amorphous solids (Hofstraat et al., 1996; Linnros et al., 1999; Jaba et al., 2000; Pophristic et al., 2000). In this study we use such an analysis as an effective and efficient description of the decay kinetics that captures both the rates (τ) and the heterogeneity (β) inherent within the decay processes. For $\beta < 1$, the fit lifetime approximately estimates the maximum in the corresponding lifetime distribution (Lindsey and Patterson, 1980).

The stretched exponential lifetimes during heating are plotted versus temperature in Fig. 5; lifetimes were identical within error during the cooling cycle (data not shown). The lifetimes decreased biphasically with increasing temperature, exhibiting a gradual linear decrease at low and a more dramatic decrease at high temperature. The decrease in lifetime with temperature reflects an increase in the rate of nonradiative decay of the excited triplet state T_1 (Eq. 6 in Materials and Methods) due to an increase in both the rate of reverse intersystem crossing to S_1 (k_{TS1}) and the rate of nonradiative decay to the ground state S_0 (k_{TS0}).

A plot of the rate constant for phosphorescence ($k_P = 1/\tau_P$), Fig. 6, was linear at low temperature and exhibited

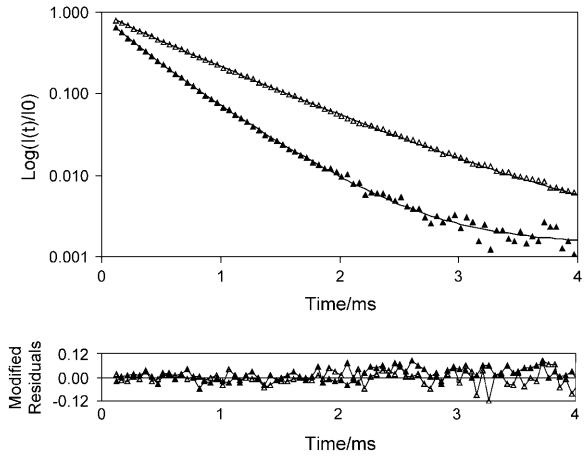

FIGURE 4 Normalized intensity decays ($I(t)/I(0)$) of erythrosin B in amorphous sucrose film at 5°C (△) and at 85°C (▲). The smooth curves through the data points are fits using a stretched exponential function with $\tau = 0.625$ ms and $\beta = 0.921$ (5°C data) and $\tau = 0.321$ ms and $\beta = 0.857$ (85°C data). The lower figure is a plot of the modified residuals for these fits.

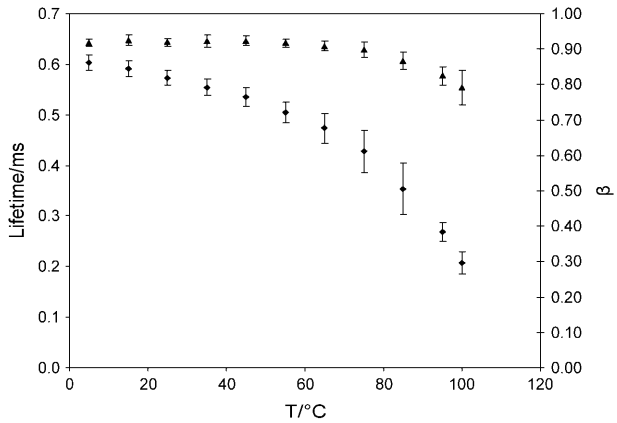

FIGURE 5 Temperature dependence of lifetimes (♦, *left* scale) and stretching exponents β (▲, *right* scale) from fits to a stretched exponential model of the intensity decay of erythrosin B in amorphous sucrose. Data collected during heating from low to high temperature.

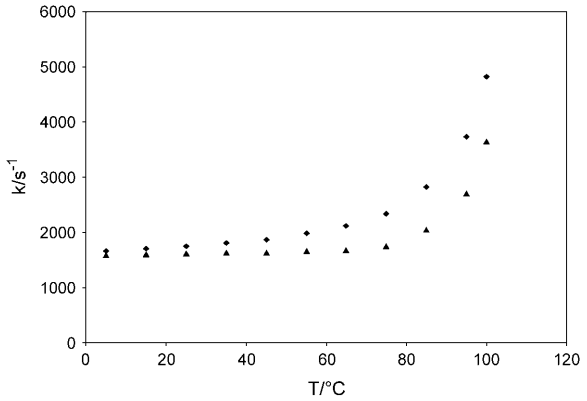

FIGURE 6 Temperature dependence of the total rate constant for nonradiative decay of the triplet state ($k = k_{RP} + k_{TS0} + k_{TS1}$) of erythrosin B in amorphous sucrose over the temperature range from 5 to 100°C (♦); values were calculated from the lifetime data in Fig. 5. An estimate of the lower limit for the rate of nonradiative decay to S_0 ($k = k_{TS0}$) is also plotted (▲); see text for additional details.

significant upward curvature at high temperature. The contribution of k_{TS1} to the phosphorescence rate constant at each temperature was estimated using the value of ΔE_{TS} determined above and various values of the preexponential constant, k^o_{TS1} (Eq. 8 in Materials and Methods). Unfortunately, literature values of k^o_{TS1} for erythrosin B vary widely, from 0.3×10^7 s^{-1} in ethanol and 6.5×10^7 s^{-1} in water (Duchowicz et al., 1998) to 111×10^7 s^{-1} in solid polyvinyl alcohol (Lettinga et al., 2000), and thus provide little guidance. Evaluation of the nonradiative decay rate k_{TS0} from k_P using $k_{RP} = 41$ s^{-1} and various estimated values of $k_{TS1}(T)$ indicated that $k^o_{TS1} \leq \sim 3 \times 10^7$ s^{-1}, as values greater than this generated a nonphysical decrease in k_{TS0} with increasing temperature from 0 to ~50°C. An estimate of the lower limit of k_{TS0}, based on the maximum physically reasonable value of k_{TS1}, is also plotted in Fig. 6.

This analysis indicates that k_{TS0}, the nonradiative quenching rate, was approximately constant at ~1600 s^{-1} in glassy sucrose, although any slight increase with temperature would be obscured by our analysis of the contribution of $k_{TS1}(T)$. This value is larger than that in ethanol (1000 s^{-1}), significantly smaller than that in water (3200 s^{-1}) (Duchowicz et al., 1998), and essentially the same as that in solid polyvinyl alcohol (1460 s^{-1}) (Lettinga et al., 2000). At temperatures near the sucrose T_g, however, k_{TS0} increased dramatically, rising to ~3500 s^{-1} in the sucrose melt at 100°C. The nonradiative quenching rate of the erythrosin triplet state, thus, effectively sensed the large-scale molecular mobility activated at the glass transition.

A plot of the stretching exponent, β, for these lifetime fits also exhibited systematic variations with temperature (Fig. 5), remaining constant at ~0.92 up to ~50°C and decreasing at higher temperatures to 0.80 at 100°C; values were essentially identical during the cooling cycle (data not shown). Even a small decrease in β reflects a large increase in the width of the distribution of phosphorescence decay times (Lindsey and Patterson, 1980). Because the distribution of decay times reflects a corresponding distribution of dynamically distinct probe environments with different values of k_{TS0}, the decrease in β indicated that the range of dynamically distinct probe environments increased above the glass transition. The range of dynamically distinct environments thus appeared to increase upon activation of the α-relaxations in the sucrose melt.

Spectral heterogeneity

The phosphorescence emission of erythrosin in amorphous sucrose exhibited a blue shift to higher energy as a function of time after excitation in both the glass and the melt (Fig. 7). Such a shift to higher emission energy with time after excitation was unexpected and cannot, for example, be explained in terms of a homogeneous relaxation model for spectral shifts (Lakowicz, 1999; Richert, 2000; Demchenko, 2002). We are aware of only one other report of a time-dependent blue shift in emission spectra, that of benzo[a]-pyrene adducts of adenine in cryogenic glass (Lin et al., 1999). Such behavior is consistent with erythrosin probes residing in spectrally distinct sites within the sucrose matrix.

Phosphorescence intensity decays were measured as a function of both excitation and emission wavelength at temperatures from 5 to 85°C to test this hypothesis. Lifetimes (from analysis using a stretched exponential model) are plotted versus excitation and emission wavelength in Fig. 8 *a*. At 5, 25, 45, and 55°C, the lifetimes decreased systematically with increasing wavelength across the emission band. Near the sucrose T_g, however, another trend became apparent as the lifetimes began to increase at intermediate wavelengths (near 660 nm). This secondary trend was more pronounced at higher temperature; by 85°C the lifetimes at 640 and 720 nm emission were identical within error whereas the lifetime at 660 nm was significantly higher. Lifetimes also varied across the excitation band, being higher

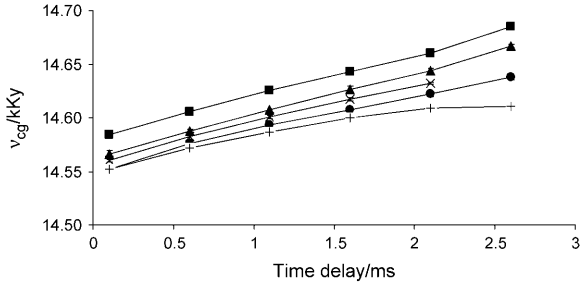

FIGURE 7 Blue shift of the phosphorescence emission spectrum of erythrosin B as a function of time after excitation in amorphous sucrose films at five temperatures below and above T_g. The center of gravity of the phosphorescence emission band collected over a 0.5-ms window is plotted versus the time delay in films at 5°C (■), 25°C (▲), 46°C (×), 60°C (●), and 76°C (+).

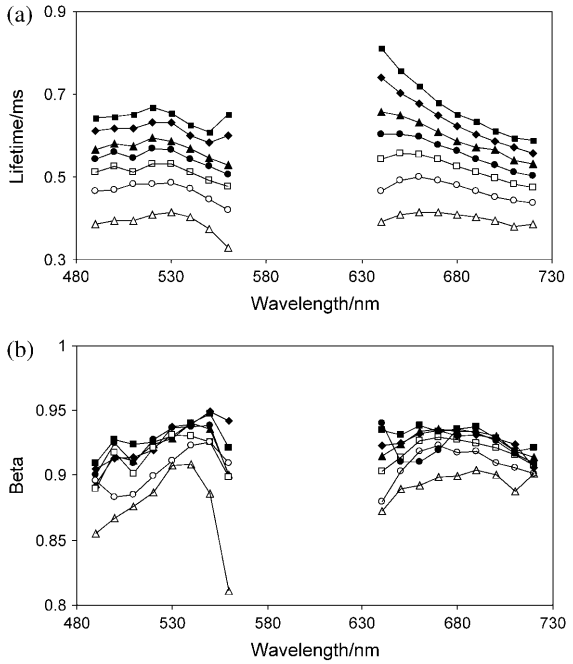

FIGURE 8 Lifetimes (*a*) and stretching exponents β (*b*) from fits to the stretched exponential model of intensity decays of erythrosin B in amorphous sucrose film collected as a function of excitation wavelength (with 680 nm emission) or emission wavelength (with 530 nm excitation). Data collected at 5°C (■), 25°C (♦), 45°C (▲), 55°C (●), 65°C (□), 75°C (○), and 85°C (△).

near the absorption maximum of 530 nm at all temperatures. Higher lifetimes were seen at the red edge of the absorption band at 560 nm only at low temperatures (5 and 25°C).

The variation in erythrosin lifetime with emission wavelength clearly indicates that molecules with blue-shifted emission spectra have longer lifetimes and molecules with red-shifted emission spectra have shorter lifetimes. A model involving ground state heterogeneity of the chromophore in which emission spectra are associated with lifetimes readily explains the blue shift seen in the emission with time (Fig. 7). At short times after excitation, the emission occurred from all species (weighted by their quantum yield and absorbance); at longer times, however, the spectra predominately reflected emission from the longer lifetime species; because the long lifetime species had a blue-shifted emission, the emission band shifted to the blue (to higher energy) as a function of time after excitation. This effect appears to obscure any red shift due to matrix relaxation around the excited triplet state.

The stretching exponent β also varied as a function of both excitation and emission wavelength (Fig. 8 *b*), being slightly smaller at the blue and red edges of both the excitation and emission bands. This trend increased at higher temperatures; at 5°C, β varied from 0.910 at 490 nm to 0.932 at 530 nm whereas at 85°C, β varied from 0.811 at 560 nm to 0.908 at 540 nm.

DISCUSSION

These spectroscopic data indicate that erythrosin phosphorescence is sensitive to thermally induced changes in the physical properties of the amorphous sucrose solid. We propose that the triplet state photophysics of erythrosin are modulated primarily by two dynamic properties of the matrix: dipolar relaxations that lower the energy of the excited triplet state and molecular motions that quench the excited triplet state. Variations in the rates of molecular mobility throughout the matrix, either through space at any given time or through time at any given site, generate site heterogeneities that further complicate the probe's spectroscopic response. Such a proposal generates, we believe, a consistent model for the triplet state photophysics of erythrosin in amorphous sucrose while providing insight into the solid-state biophysics of amorphous sugars.

Dipolar relaxation

The phosphorescence emission energy, monitored here either as maximum emission frequency or center of gravity of the emission band, reports the average S_0-T_1 energy gap; within the polar sucrose matrix, this gap is primarily modulated by the T_1 energy and thus by the relaxation of dipolar hydroxyl groups around T_1 (Richert, 2000). Temperature had a small effect on the emission energy within the sucrose glass and a much larger effect in the melt above T_g; the relaxation rate thus increased significantly in the sucrose melt, presumably due to activation of translational motions at T_g, α-relaxations, that facilitate dipolar relaxation mechanisms (involving motions ranging from local rotation of –OH groups to the rotation of entire molecules).

Temperature had a similar influence on the magnitude of the red-edge effect. The emission energy difference with excitation at the peak and at the red edge decreased gradually in the glass below T_g and more steeply in the melt above T_g. Because this energy difference reflects the persistence of low-energy sites photoselected by low-energy excitation (Demchenko, 2002), the decay of the energy difference above T_g reflects an increase in the rate of matrix relaxation that equilibrates the energy of all sites on the lifetime of the triplet state.

The proposal that dipolar relaxation within the sucrose matrix modulates the phosphorescence emission energy of erythrosin is hardly controversial for either phosphorescence (Richert, 2000) or fluorescence (Ware et al., 1971; Stratt and Maroncelli, 1996). For erythrosin in sucrose, however, emission spectra did not relax to lower energy as a function of time after excitation but rather blue-shifted to higher energy. Such anomalous behavior requires a more complicated photophysical model that correlates emission spectra with triplet state lifetime.

Collisional quenching

Our analysis of the effect of temperature on lifetime indicates that the nonradiative quenching rate increased dramatically in the melt above T_g. The exact mechanism of this additional quenching is obscure—in large part because quenching mechanisms for the triplet state of erythrosin and other probes are poorly understood—but reflects either the increase of an existing quenching pathway or the activation of a novel quenching pathway. Either mechanism involves an increase in the ability of the excited erythrosin to dissipate vibrational energy into the matrix. It is clear from the decrease of the lifetime with temperature that such dissipation is facilitated by the α-relaxations activated at T_g; in other words, that there is effective coupling between matrix α-relaxations and vibrational motions of the probe.

The variation of lifetime with emission wavelength reflects variation in one or more of the rate constants for deexcitation of the triplet state. We can evaluate the possible contributions of these rate constants using qualitative arguments. The intrinsic emission rate, k_{RP}, which varies with the third power of the emission energy ($k_{RP} \propto \nu^3$) (Cantor and Schimmel, 1980), is expected to decrease with decreasing emission energy; this would cause an increase in the lifetime with increasing wavelength rather than the decrease observed. The reverse intersystem crossing rate is sensitive to the S_1-T_1 energy gap (ΔE_{TS}), $k_{TS1} \propto \exp(-\Delta E_{TS}/RT)$; an increase in ΔE_{TS} would thus decrease this rate constant. Probes emitting at longer wavelength would be expected to have larger S_1-T_1 energy gaps (due to lower T_1 energy) and thus lower values of k_{TS1}; this would cause an increase in lifetime with increasing wavelength rather than the decrease seen. The decrease in lifetime with emission wavelength must thus reflect a variation in the nonradiative quenching rate, k_{TS0}, with wavelength. There is, thus, a correlation between emission energy and matrix quenching rate among probes within the amorphous solid: probes with higher emission energy have lower matrix quenching rate and probes with lower emission energy have higher matrix quenching rate. Variations in lifetime with excitation wavelength provide evidence that these probes also have distinct absorption bands.

This analysis indicates that it is appropriate to calculate the wavelength dependence of the apparent activation energies (E_A) for matrix (nonradiative) quenching in the glass below and the melt above T_g. Activation energies, calculated from Arrhenius plots at temperatures below and above T_g, are plotted in Fig. 9. In both the glass and in the melt, the values of E_A were higher for probes with blue-shifted emission and red-shifted absorption. The activation energy, thus, also exhibited spectral heterogeneity in amorphous sucrose; probes in higher energy sites with lower matrix quenching rates also had higher activation energies for the motions that quench the triplet state.

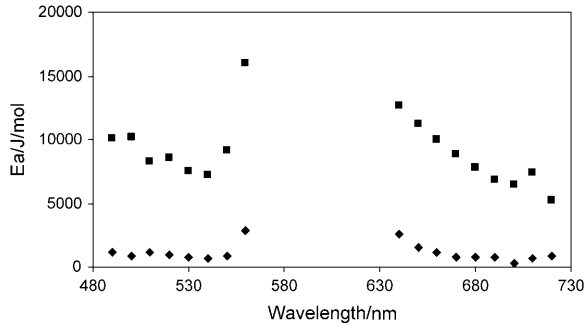

FIGURE 9 Apparent activation energy (E_A) for nonradiative decay rate of erythrosin B in the sucrose glass (♦) below and melt (■) above T_g as a function of excitation and emission wavelength (calculated from an Arrhenius analysis of the data in Fig. 8 *a* using the three lowest and highest temperatures, respectively).

Dynamic site heterogeneity

The observed correlation of emission energy with matrix quenching rate cannot reflect the behavior of a homogeneous population of probes simultaneously undergoing emission and relaxation to lower energy. Rather, it appears to reflect the behavior of a heterogeneous population of probes distributed among dynamically distinct sites within the sucrose matrix that vary in both emission energy and matrix quenching rate. The success of a stretched exponential function with $\beta \approx 0.8$–0.9 to describe the phosphorescence decay suggests that a continuum of sites, rather than a limited set of distinct sites, gives rise to the heterogeneity. A reasonable physical model for the origin of this site heterogeneity invokes local differences in packing interactions among molecules within the amorphous sucrose. Local environments with more constrained/tighter packing (due perhaps to more extensive hydrogen bonding) would have lower overall molecular mobility; probes in such lower mobility environments would have longer lifetimes due to slower/fewer molecular collisions that quench the triplet state, higher emission energy due to slower/less extensive dipolar relaxation around the excited triplet state, and higher activation energies for nonradiative decay due to more constraints on motion(s) within the sucrose matrix. Local environments with less constrained/looser packing (due perhaps to less extensive hydrogen bonding) would have higher overall molecular mobility; probes in such higher mobility environments would have shorter lifetimes due to faster/more molecular collisions that quench the triplet state, lower emission energy due to faster/more extensive dipolar relaxation around the excited triplet state, and lower activation energies for nonradiative decay due to fewer constraints on motion(s) within the sucrose matrix. These dynamically distinct sites persist for times significantly longer than 0.5 ms, the excited state lifetime of erythrosin. Our data do not allow us to calculate a persistence time for these sites.

The magnitude of the variation in lifetime with wavelength decreased at higher temperature, but the emission blue shift with time persisted even at 76°C (Fig. 8 *a*), suggesting that spectral heterogeneity may have decreased but did not disappear altogether in the melt. In addition, above T_g, the emission bandwidth increased (Fig. 2), indicating that the distribution of site energies broadened, and the stretching exponent β decreased (Fig. 5), indicating that the distribution of matrix quenching rates broadened; there was thus a significant broadening in the distribution of dynamic environments in the sugar melt. The decrease in the spectral heterogeneity above T_g may reflect an actual decrease in site heterogeneity (increase in site homogeneity) within the amorphous sucrose or it may merely reflect the loss of the probe's ability to report site heterogeneity; if so, the loss of the ability to report site heterogeneity may be the result of broadening in the distribution of site energies and quenching rates.

Dynamic heterogeneity in supercooled liquids

Recent research indicates that supercooled liquids are dynamically heterogeneous both spatially and temporally (see, for example, detailed reviews by Sillescu, 1999; Ediger, 2000; Richert, 2002). Multidimensional NMR (Schmidt-Rohr and Spiess, 1991) and extensive photobleaching of optical probes (Cicerone and Ediger, 1993) have been used to directly monitor slower relaxation rates of spectrally selected dynamic subensembles within the supercooled liquid or amorphous solid; both techniques are also able to determine the timescale (referred to as the rate memory or rate exchange) required for the relaxation times of the subensemble to redistribute to those of the full ensemble (Heuer et al., 1995; Wang and Ediger, 1999). Dielectric hole burning, which detects dynamic heterogeneity by altering the polarization response of dynamic subensembles in a spectrally selective manner (Schiener et al., 1996), has been used to detect heterogeneity within the α-relaxation in supercooled molecular liquids (Schiener et al., 1997) and within the Johari-Goldstein β-relaxation in the glassy sugar alcohol sorbitol (Richert, 2001a), among other systems. The persistence time of spectral holes also provides information about rate exchange.

Solvation dynamics around the excited state of triplet chromophores has been used by Richert and colleagues to measure both the rate and heterogeneity of matrix relaxation in supercooled liquids; heterogeneity is detected through time dependent measurements of the spectral linewidth during solvation (Richert, 1997; Richert and Richert, 1998). A quantitative theory indicates that heterogeneity reveals itself as a maximum in the time-dependent linewidth (Richert, 2001b); analysis of linewidth can also provide information about rate exchange (Richert, 2001c). Studies of triplet state solvation dynamics in a variety of supercooled and glassy systems (Richert, 2000) indicate that dynamic heterogeneity among sites with exponential solvation behavior gives rise to the stretched exponential ($\beta < 1$) solvation dynamics observed in these systems.

The results described here indicate that the emission (and perhaps excitation) dependence of the intensity decay from erythrosin, and other triplet probes, also provides information about the dynamic heterogeneity within supercooled liquids and amorphous solids. We have seen similar coupling of lifetimes with emission energy in the phosphorescence spectra of erythrosin in other sugars (Shirke, 2005) and in amorphous gelatin (Lukasik, 2004), eosin in amorphous sucrose (Pravinata, 2003) and amorphous gelatin (Lukasik, 2004), and of tryptophan amino acid in amorphous sugars (Zunić, 2004), suggesting that the phenomenon may be commonplace in amorphous biomaterials. The ability to independently monitor sites of different mobility within amorphous solids using yet another spectroscopic technique allows for a far more detailed dissection of the complex dynamic properties of amorphous biomaterials.

The authors thank Drs. Alexander Demchenko and Catherine Royer for comments helpful in the analysis of the blue-shift in emission spectra with time.

This is publication No. D-10544-4-03 of the New Jersey Agricultural Experiment Station supported by state funds, the Center for Advanced Food Technology, the National Research Initiative of the U.S. Department of Agriculture (No. 2001-01683), and the Mid-Atlantic Consortium supported by the Kellogg Foundation.

REFERENCES

Buitink, J., and L. Olivier. 2004. Glass formation in plant anhydrobiotes: survival in the dry state. *Cryobiology*. 48:215–228.

Buitink, J., I. J. Van den Dries, F. A. Hoekstra, M. Alberda, and M. A. Hemminga. 2000. High critical temperature above T_g may contribute to the stability of biological systems. *Biophys. J.* 79:1119–1128.

Cantor, C. R., and P. R. Schimmel. 1980. Biophysical Chemistry, Part II: Techniques of the Study of Biological Structure and Function. W. H. Freeman & Co., San Francisco, CA.

Carstensen, J. T. 2000. Solid state stability. *Drugs Pharm. Sci.* 107:145–189.

Cicerone, M. T., and M. D. Ediger. 1993. Photobleaching technique for measuring ultraslow reorientation near and below the glass transition: tetracene in *o*-terphenyl. *J. Chem. Phys.* 97:10489–10497.

Craig, D. Q., P. G. Royall, V. L. Kett, and M. L. Hopton. 1999. The relevance of the amorphous state to pharmaceutical dosage forms: glassy drugs and freeze-dried systems. *Int. J. Pharm.* 179:179–207.

Crowe, J. H., J. F. Carpenter, and L. M. Crowe. 1998. The role of vitrification in anhydrobiosis. *Annu. Rev. Physiol.* 60:73–103.

Crowe, J. H., A. E. Oliver, and F. Tablin. 2002. Is there a single biochemical adaptation to anhydrobiosis? *Integrat. Comp. Biol.* 42:497–503.

Demchenko, A. P. 2002. The red-edge effect: 30 years of exploration. *Luminescence*. 17:19–42.

Doye, J. P. K., A. A. Louis, and M. Vendruscolo. 2004. Inhibition of protein crystallization by evolutionary negative design. *Physical Biol.* 1:P9–P13.

Duchowicz, R., M. L. Ferrer, and A. U. Acuna. 1998. Kinetic spectroscopy of erythrosin phosphorescence and delayed fluorescence in aqueous solution at room temperature. *Photochem. Photobiol.* 68:494–501.

Ediger, M. D. 2000. Spatially heterogeneous dynamics in supercooled liquids. *Annu. Rev. Phys. Chem.* 51:99–128.

Fennema, O. 1996. Water and ice. *In* Food Chemistry, 3rd Ed. O. Fennema, editor. Marcel Dekker, New York.

Galley, W. C., and R. M. Purkey. 1970. Role of heterogeneity of the solvation site in electronic spectra in solution. *Proc. Natl. Acad. Sci. USA.* 67:1116–1121.

Heuer, A., M. Wilhelm, H. Zimmerman, and H. W. Spiess. 1995. Rate memory of structural relaxation in glasses and its detection by multidimensional NMR. *Phys. Rev. Lett.* 75:2851–2854.

Hofstraat, J. W., H. J. Verhey, J. W. Verhoeven, M. U. Kumke, L. B. McGown, E. G. Novikov, A. van Hoek, and A. J. W. G. Visser. 1996. Time-resolved spectroscopy of charge-transfer fluorescent molecules in polymer matrixes. *Proc. SPIE.* 2705:110–121.

Jaba, N., A. Kanoun, H. Mejri, H. Maaref, and A. Brenier. 2000. Time-resolved luminescence data on the 1060 nm transition in Nd^{3+}-doped zinc tellurite glasses. *J. Phys. Condens. Matter.* 12:7303–7309.

Johari, G. P., and M. Goldstein. 1970. Viscous liquids and the glass transition. II. Secondary relaxations in glasses of rigid molecules. *J. Chem. Phys.* 53:2372–2388.

Johari, G. P., and M. Goldstein. 1971. Viscous liquids and the glass transition. III. Secondary relaxations in aliphatic alcohols and other nonrigid molecules. *J. Chem. Phys.* 55:4245–4252.

Karel, M., and I. Saguy. 1991. Effects of water on diffusion in food systems. *Adv. Exp. Med. Biol.* 302:157–173.

Lakowicz, J. R. 1999. Principles of Fluorescence Spectroscopy. Plenum Press, New York.

Leopold, C. A. 1999. Survival of seeds in the dry state. *Rev-R. Acad. Galega Cienc.* 18:5–18.

Lettinga, M. P., H. Zuilhof, and A. M. J. van Zandvoort. 2000. Phosphorescence and fluorescence characterization of fluorescein derivatives immobilized in various polymer matrices. *Phys. Chem. Chem. Phys.* 2:3697–3707.

Lin, C.-H., D. Zamzow, G. J. Small, and R. Jankowiak. 1999. Time-dependent blue shift of the fluorescence origin band of benzo[a]pyrene (BP)-derived BP-6–N7Ade adducts in glasses. *Polycylic. Arom. Comp.* 14/15:43–52.

Lindsey, C. P., and G. D. Patterson. 1980. Detailed comparison of the Williams-Watts and Cole-Davidson functions. *J. Chem. Phys.* 73:3348–3357.

Linnros, J., N. Lalic, A. Galeckas, and V. Grivickas. 1999. Analysis of the stretched exponential photoluminescence decay from nanometer-sized silicon crystals in SiO_2. *J. Appl. Phys.* 86:6128–6134.

Ludescher, R. D., N. K. Shah, C. P. McCaul, and K. V. Simon. 2001. Beyond Tg: optical luminescence measurements of molecular mobility in amorphous solid foods. *Food Hydrocolloids.* 15:331–339.

Lukasik, K. V. 2004. Luminescent probes of structural and dynamic heterogeneity in gelatin. PhD dissertation. Rutgers University, New Brunswick, NJ.

Maroncelli, M., and G. R. Fleming. 1987. Picosecond solvation dynamics of coumarin 153: the importance of molecular aspects of solvation. *J. Chem. Phys.* 86:6221–6239.

McCrum, N. G., B. E. Read, and G. Williams. 1967. Anelastic and dielectric effects in polymeric solids. John Wiley & Sons, New York.

Pant, D. D., C. L. Bhagchandani, K. C. Pant, and S. P. Verma. 1971. Aggregation of xanthene dyes: exciton emission and phosphorescence enhancement. *Chem. Phys. Lett.* 9:546–547.

Papp, S., and J. M. Vanderkooi. 1989. Tryptophan phosphorescence at room temperature as a tool to study protein structure and function. *Photochem. Photobiol.* 49:775–784.

Parker, C. A. 1968. Photoluminescence of Solutions. Elsevier Publishing, Amsterdam, The Netherlands.

Peleg, M. 1996. On modeling changes in food and biosolids at and around the glass transition temperature range. *Crit. Rev. Food Sci. Nutr.* 36: 49–67.

Pophristic, M., S. J. Lukacs, F. H. Long, C. A. Tran, and I. T. Ferguson. 2000. Disorder in InGaN light-emitting diodes. *Proc. SPIE.* 3938: 105–112.

Pravinata, L. C. 2003. Molecular mobility of amorphous sucrose detected by phosphorescence of erythrosin B and eosin Y. Masters thesis. Rutgers University, New Brunswick, NJ.

Richert, R. 1997. Evidence for dynamic heterogeneity near T_g for the time resolved inhomogeneous broadening of optical line shapes. *J. Phys. Chem. B.* 101:6323–6326.

Richert, R. 1998. Molecular dynamics analyzed in terms of continuous measures of dynamic heterogeneity. *J. Non-Cryst. Solids.* 235–237: 41–47.

Richert, R. 2000. Triplet state solvation dynamics: basics and applications. *J. Chem. Phys.* 113:8404–8429.

Richert, R. 2001a. Spectral selectivity in the slow β-relaxation of a molecular glass. *Europhys. Lett.* 54:767–773.

Richert, R. 2001b. Theory of time dependent optical linewidths in supercooled liquids. *J. Chem. Phys.* 114:7471–7476.

Richert, R. 2001c. Spectral diffusion in liquids with fluctuating solvent responses: dynamical heterogeneity and rate exchange. *J. Chem. Phys.* 115:1429–1434.

Richert, R. 2002. Heterogeneous dynamics in liquids: fluctuations in space and time. *J. Phys. Condens. Matter.* 14:R703–R738.

Richert, R., and M. Richert. 1998. Dynamic heterogeneity, spatially distributed stretched-exponential patterns, and transient dispersions in solvation dynamics. *Phys. Rev. E.* 58:779–784.

Roos, Y. 1995. Phase Transitions in Foods. Academic Press, San Diego, CA.

Schauerte, J. A., D. G. Steele, and A. Gafni. 1997. Time-resolved room temperature phosphorescence in proteins. *Methods Enzymol.* 278: 49–71.

Schiener, B., R. Böhmer, A. Loidl, and R. V. Chamberlin. 1996. Nonresonant spectral hole burning in the slow dielectric response of supercooled liquids. *Science.* 274:752–754.

Schiener, B., R. V. Chamberlin, G. Diezemann, and R. Böhmer. 1997. Nonresonant dielectric hole burning spectroscopy of supercooled liquids. *J. Chem. Phys.* 107:7746–7761.

Schmidt-Rohr, K., and H. W. Spiess. 1991. Nature of the nonexponential loss of correlation above the glass transition investigated by multidimensional NMR. *Phys. Rev. Lett.* 66:3020–3023.

Shah, N. K., and R. D. Ludescher. 1994. Influence of hydration on the internal dynamics of hen egg white lysozyme in the dry state. *Photochem. Photobiol.* 58:169–174.

Shah, N. K., and R. D. Ludescher. 1995. Phosphorescence probes of the glassy state in amorphous sucrose. *Biotechnol. Prog.* 11:540–544.

Shirke, S. 2005. Molecular mobility of sugars and sugar alcohols as detected by phosphorescence of erythrosin B. Masters thesis. Rutgers University, New Brunswick, NJ.

Sillescu, H. 1999. Heterogeneity at the glass transition: a review. *J. Non-Cryst. Solids.* 243:81–108.

Skrabanja, A. T., A. L. de Meere, R. A. de Ruiter, and P. J. van den Oetelaar. 1994. Lyophilization of biotechnology products. *PDA J. Pharm. Sci. Technol.* 48:311–317.

Slade, L., and H. Levine. 1995. Glass transitions and water-food structure interactions. *Adv. Food Nutr. Res.* 38:103–269.

Stratt, R. M., and M. Maroncelli. 1996. Nonreactive dynamics in solution: the emerging molecular view of solvation dynamics and vibrational relaxation. *J. Phys. Chem.* 100:12981–12996.

Sun, W. Q., P. Davidson, and H. S. O. Chan. 1998. Protein stability in the amorphous carbohydrate matrix: relevance to anhydrobiosis. *Biochim. Biophys. Acta.* 1425:245–254.

Towns, J. K. 1995. Moisture content in proteins: its effects and measurement. *J. Chromatogr. A.* 705:115–127.

Tunnacliffe, A., and J. Lapinski. 2003. Resurrecting van Leewenhoek's rotifers: a reappraisal of the role of disaccharides in anhydrobiosis. *Philos. Trans. R. Soc. Lond. B. Biol. Sci.* 358:1755–1771.

Vanderkooi, J. M., G. Maniara, T. J. Green, and D. F. Wilson. 1987. An optical method for measurement of dioxygen concentration based on quenching of phosphorescence. *J. Biol. Chem.* 262:5476–5482.

Ware, W. R., S. K. Lee, G. J. Brant, and P. P. Chow. 1971. Nanosecond time-resolved emission spectroscopy: spectral shifts due to solvent-excited solution relaxation. *J. Chem. Phys.* 54:4729–4737.

Wang, C.-Y., and M. D. Ediger. 1999. How long do regions of different dynamics persist in supercooled ortho-terphenyl? *J. Phys. Chem. B.* 103:4177–4184.

Zallen, R. 1983. The Physics of Amorphous Solids. John Wiley & Sons, New York.

Zunić, A. 2004. Molecular Mobility of Amorphous Disaccharides Studied by Tryptophan Luminescence. Masters thesis. Rutgers University, New Brunswick, NJ.